Journal of Alloys and Compounds 434–435 (2007) 217–220

Journal of ALLOYS AND COMPOUNDS

www.elsevier.com/locate/jallcom

Effect of Zr on the crystallization behavior of multi-component Zr-based metallic glasses

Sergio Scudino [a,*], Jürgen Eckert [b], Hergen Breitzke [c], Klaus Lüders [c], Ludwig Schultz [a]

[a] *IFW Dresden, Institut für Metallische Werkstoffe, Postfach 270016, D-01171 Dresden, Germany*
[b] *FG Physikalische Metallkunde, FB 11 Material- und Geowissenschaften, Technische Universität Darmstadt, Petersenstraße 23, D-64287 Darmstadt, Germany*
[c] *Fachbereich Physik, Freie Universität Berlin, Arnimallee 14, D-14195 Berlin, Germany*

Available online 16 October 2006

Abstract

Melt-spun $Zr_y(Ti_{0.186}Nb_{0.058}Cu_{0.324}Ni_{0.258}Al_{0.174})_{100-y}$ glassy ribbons with $y = 57$ and 62 were investigated by differential scanning calorimetry, X-ray diffraction and transmission electron microscopy in order to clarify the role of Zr on the crystallization behavior. The devitrification of the ribbons is characterized by the formation of a metastable icosahedral quasicrystalline phase during the first stage of the crystallization process. With increasing amount of Zr the thermal stability against crystallization decreases whereas the temperature range of stability of the quasicrystalline phase increases. Furthermore, the grain size and the volume fraction of the quasicrystalline precipitates increases with increasing Zr content. Accordingly, appropriately adjusting the Zr content allows for tuning the thermal stability as well as the microstructure evolution upon heating.

Keywords: Metallic glasses; Quasicrystals; Rapid-solidification

1. Introduction

The amorphous-to-quasicrystalline phase transformation upon devitrification of $Zr_{57}Ti_8Nb_{2.5}Cu_{13.9}Ni_{11.1}Al_{7.5}$ glassy ribbons is a primary reaction (i.e. crystallization of a phase with a different composition than the amorphous matrix) characterized by the redistribution of Al and Zr between the parent amorphous phase and the arising quasicrystals [1]. Al is slightly depleted and Zr is slightly enriched in the nanosized quasicrystalline precipitates. Therefore, the diffusion of these elements is an essential aspect of the mechanism of quasicrystalline phase formation in this alloy, suggesting the possibility to tune the thermal stability and the microstructure evolution of the glass by changing the amount of Al and/or Zr. For example, by increasing or decreasing the Zr content, the formation of quasicrystals may be assisted or depressed, respectively. This behavior is important not only from a scientific point of view, i.e. in order to understand the effect of composition on the formation of quasicrystals, but it has also significant consequences on the possible engineering applications of this glassy alloy as precursor for nanocomposites materials [2]. In fact, it has been reported that the microstructure of nanosized particles embedded in a glassy matrix yields high strength and good ductility when the volume fraction is less than about 40% [3,4]. In contrast, particles of micrometer size have a strong effect on crack initiation leading to early fracture [5]. Consequently, the ability to produce a controlled microstructure is a prerequisite for commercial application. Another fundamental aspect that has to be taken into account is the stability of quasicrystals (QC). The utilization of a partially devitrified material requires a wide temperature interval between the formation of the primary phase and the subsequent transformation events. Chemical composition has a strong influence on both thermal stability and microstructure evolution upon heating [6,7] and, thus, the knowledge of the influence of composition on both these features is extremely important. Accordingly, in this work the influence of the Zr content on the crystallization behavior of melt-spun $Zr_{57}Ti_8Nb_{2.5}Cu_{13.9}Ni_{11.1}Al_{7.5}$ glassy ribbons has been investigated.

2. Experimental

Prealloyed ingots with nominal composition $Zr_y(Ti_{0.186}Nb_{0.058}Cu_{0.324}Ni_{0.258}Al_{0.174})_{100-y}$ ($y = 57$ and 62) were prepared from pure elements (purity > 99.9 wt.%) by arc melting in a titanium-gettered argon atmosphere. The ingots were remelted several times in order to achieve homogeneity in com-

* Corresponding author. Present address: FG Physikalische Metallkunde, FB 11 Material- und Geowissenschaften, Technische Universität Darmstadt, Petersenstraße 23, D-64287 Darmstadt, Germany. Tel.: +49 6151 16 5596; fax: +49 6151 16 5557.
E-mail address: s.scudino@phm.tu-darmstadt.de (S. Scudino).

0925-8388/$ – see front matter © 2006 Elsevier B.V. All rights reserved.
doi:10.1016/j.jallcom.2006.08.162

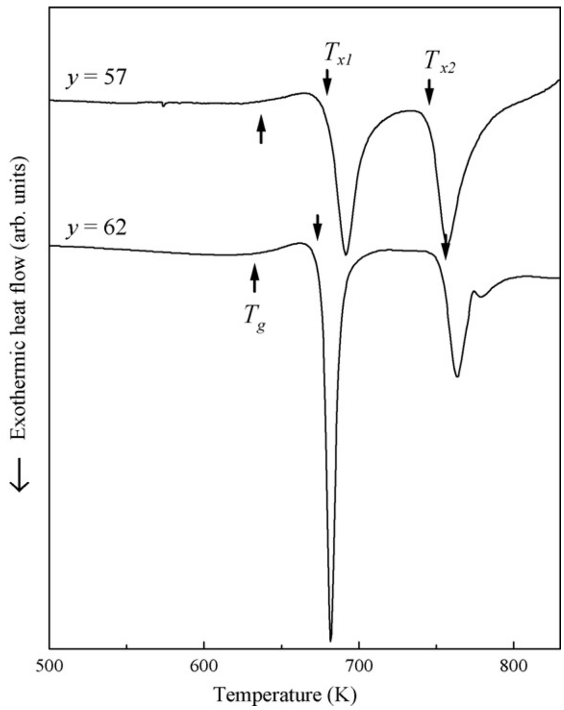

Fig. 1. Constant-rate heating DSC (40 K/min) scans of the melt-spun $Zr_y(Ti_{0.186}Nb_{0.058}Cu_{0.324}Ni_{0.258}Al_{0.174})_{100-y}$ glassy ribbons with $y = 57$ and 62.

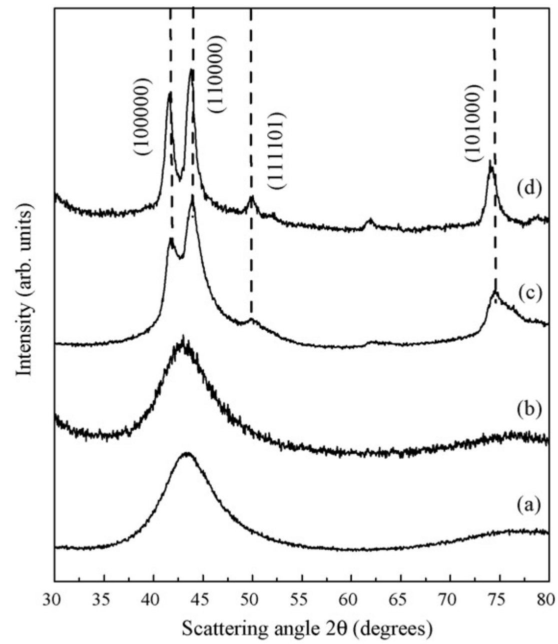

Fig. 2. XRD patterns (Co-Kα radiation) for the as-spun ribbons with (a) $y = 57$ and (b) $y = 62$, and for the ribbons heated up to the completion of the first exothermic DSC peak (c) $y = 57$ and (d) $y = 62$.

position. Ribbons with a cross section of about 0.05 mm × 3 mm were prepared in a single-roller Bühler melt spinner at a wheel velocity of 14.3 m/s under an argon atmosphere. Since oxygen contamination may influence the crystallization behavior [8–10], special care was taken to ensure a comparable amount of oxygen in both ribbons. This amount, evaluated by carrier gas hot extraction using a Leco TC-436DR analyzer, was found to be about 0.05 wt.%. The microstructure was characterized by X-ray diffraction (XRD) using a Philips PW 1050 diffractometer (Co-Kα radiation) and by transmission electron microscopy (TEM) using a Philips CM 20 microscope. The thermal stability of the samples was investigated by differential scanning calorimetry (DSC) at 40 K/min heating rate with a Perkin-Elmer DSC7 under a continuous flow of purified argon.

3. Results and discussion

Fig. 1 shows the constant-rate heating DSC scans (40 K/min) of the melt-spun glassy ribbons with $y = 57$ and 62. Both DSC curves exhibit the same general behavior, namely, a distinct glass transition followed by two crystallization events at higher temperatures. The effect of Zr on the thermal stability data evaluated from Fig. 1 is summarized in Table 1. The temperature of the glass transition (T_g) and the crystallization temperature related to the first crystallization event (T_{x1}) shift to lower values by about 10 and 20 K, respectively, with increasing Zr content. Therefore, varying the composition strongly affects the devitrification by lowering the temperature of the transformation from the solid state glass to the supercooled liquid (SCL) and by decreasing the stability of the SCL against crystallization. The variation of T_g and T_{x1} gives rise to a decrease of the supercooled liquid region ($\Delta T_{x1} = T_{x1} - T_g$) of about 10 K when increasing the Zr content from $y = 57$ to 62.

When partially crystallized materials are considered, a fundamental parameter that has to be considered is the temperature range of stability of the phase formed, which in the present case is $\Delta T_{x2} = T_{x2} - T_{x1}$, i.e. the temperature interval between the first crystallization temperature, where the primary phase forms, and the subsequent crystallization event. ΔT_{x2} increases by about 25 K for the alloy with $y = 62$ compared to the sample with $y = 57$.

These results suggest that if one is interested in the amorphous material it is better to choose the alloy with the lower Zr content, in which the glassy phase is more stable. On the other hand, if partially crystallized material is required, the ribbons with the higher Zr content is the better choice, since it is characterized by a wider temperature range of stability of the primary precipitating phase. Finally, while the crystallization enthalpy ΔH_1 increases with increasing Zr content (approximately from 20 up to 30 J/g), indicating an increase of the quasicrystalline volume fraction formed, the same variation of composition has only a limited effect on ΔH_2, which is decreased by about 2 J/g.

The XRD patterns of the as-spun ribbons (Fig. 2(a) and (b)) exhibit the typical broad diffuse maxima characteristic of amor-

Table 1
Temperature of the glass transition (T_g), onset of the first (T_{x1}) and the second (T_{x2}) crystallization peak, extension of the supercooled liquid region ($\Delta T_x = T_{x1} - T_g$), temperature range of stability of the quasicrystalline phase ($\Delta T_{x2} = T_{x2} - T_{x1}$) and crystallization enthalpies (ΔH_{x1}, ΔH_{x2}) for the melt-spun $Zr_y(Ti_{0.186}Nb_{0.058}Cu_{0.324}Ni_{0.258}Al_{0.174})_{100-y}$ glassy ribbons with $y = 57$ and 62

	T_g (K)	T_{x1} (K)	T_{x2} (K)	ΔT_{x1} (K)	ΔT_{x2} (K)	ΔH_{x1} (J/g)	ΔH_{x2} (J/g)
Ribbon with $y = 57$	646	696	748	50	52	19.1	19.9
Ribbon with $y = 62$	637	677	753	40	76	29.8	17.9

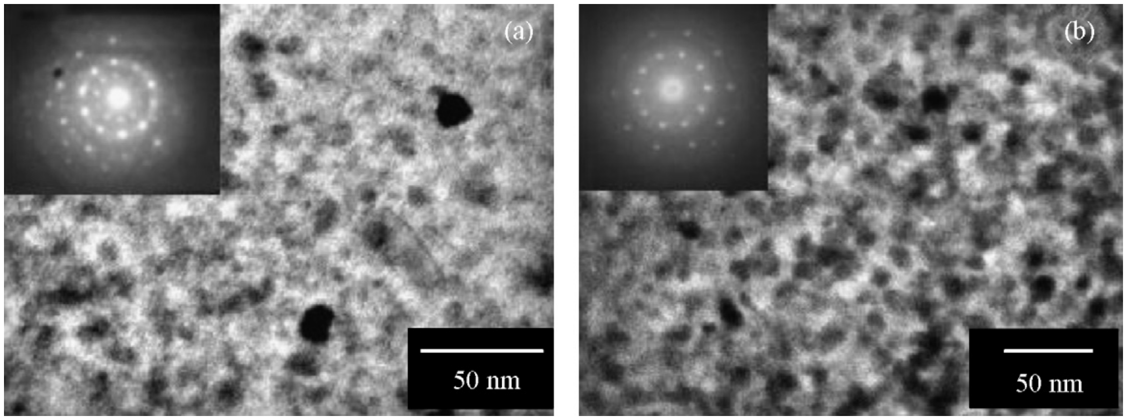

Fig. 3. Bright-field TEM images of the $Zr_y(Ti_{0.186}Nb_{0.058}Cu_{0.324}Ni_{0.258}Al_{0.174})_{100-y}$ ribbons with (a) $y=57$ and (b) $y=62$ heated to completion of the first exothermic DSC event and corresponding electron nanodiffraction patterns (insets).

phous materials and no traces of crystalline phases. In order to study the structural evolution during heating, the ribbons with $y=57$ and 62 were annealed in the DSC by continuous heating at 40 K/min up to different temperatures up to the completion of the first exothermic DSC event and then cooling to room temperature at 100 K/min. The phases formed were identified by X-ray diffraction and their patterns are shown in Fig. 2(c) and (d). Both glassy ribbons with different composition devitrify by precipitation of an icosahedral quasicrystalline phase that can be indexed according to the scheme of Bancel et al. [11]. With increasing Zr content the QC diffraction peaks sharpen, suggesting an increase of the grain size of the quasicrystals.

Fig. 3(a) and (b) shows the bright-field TEM images and the corresponding electron diffraction patterns of the samples with $y=57$ and 62, respectively, after heating at 40 K/min up to the completion of the first crystallization event. The micrographs reveal a homogeneous distribution of particles. While the particles precipitated in the alloy with $y=57$ have a size on the order of 5–10 nm, in the samples with $y=62$ the dimensions of the quasicrystalline particles are about 10–20 nm. The electron nanodiffraction patterns taken from the precipitated particles are presented in the insets in Fig. 3(a) and (b). The patterns clearly exhibit five-fold symmetry. These findings confirm the XRD results, corroborating that the particles precipitated during the first crystallization event have a quasicrystalline structure and that increasing the Zr content yield larger QC grains. The crystallized volume fraction, estimated from the TEM images, was found to be about 40–50 vol.% for the material with $y=62$. This value is larger than for the sample with $y=57$, which comprises a volume fraction of 20–30 vol.% after the primary devitrification step. This supports the earlier assumption based on the analysis of the crystallization enthalpies, which suggested an increase of the QC volume fraction with increasing Zr content.

The reduced thermal stability against crystallization and the increased size of the quasicrystalline precipitates observed when the amount of Zr is increased might be attributed to the enhanced ease of precipitation of the quasicrystalline phase from the supercooled liquid. Crystallization only takes place when the composition of a region of the size of a critical nucleus has the composition of the nucleating phase. If the supercooled liquid has a different composition with respect to that of the quasicrystalline phase, nucleation requires a significant atomic diffusion and redistribution and, therefore, the probability to achieve a critical nucleus of the required composition is reduced. The formation of quasicrystals in the ribbon with $y=57$ requires the enrichment in Zr of the nucleating phase up to a content of about 61.7 wt.% [1]. The increase of Zr content favors the formation of the quasicrystalline phase because it reduces the amount of Zr that has to diffuse from the glassy phase/SCL to the arising quasicrystals. As a result, the formation of quasicrystals for the Zr-rich alloy may be shifted to a lower temperature. In the alloy with $y=62$ the dimensions of the quasicrystalline grains are larger than in the sample with $y=57$. This suggests a higher growth rate for the $y=62$ alloy. Growth rates can be enhanced or depressed depending on the type of crystallization mechanism [12]. For example, primary crystallization reactions, which require long-range diffusion, are inherently more complex than a polymorphous transformation that involves only local topological atomic rearrangements, and thus are expected to give the finest microstructure [13]. Although for the alloy with $y=62$ the amorphous-to-quasicrystalline transformation may still be primary, the increase of Zr reduces the required amount of redistribution of Zr between the growing quasicrystalline grains and the parent glassy phase/SCL. Most likely, this has a positive effect on the growth rate and, consequently, increases the dimensions of the quasicrystalline precipitates.

4. Conclusions

The variation of Zr strongly affects the crystallization behavior of melt-spun $Zr_y(Ti_{0.186}Nb_{0.058}Cu_{0.324}Ni_{0.258}Al_{0.174})_{100-y}$ ($y=57$ and 62) glassy ribbons. With increasing Zr content the thermal stability against crystallization decreases by about 20 K together with a decrease of the extension of the supercooled liquid region by about 10 K. However, increasing the Zr content has a positive effect on the temperature range of stability of the quasicrystalline phase that increases by about 25 K, and on the quasicrystalline volume fraction, which increases by about 20%.

Acknowledgements

The authors would like to thank M. Frey and H. Schulze for technical assistance, J. Acker and W. Gruner for chemical analysis, C. Mickel and J. Thomas for help with the TEM investigations, and B. Bartusch, U. Kühn and S. Venkataraman for stimulating discussions. This work was supported by the German Science Foundation under grants Ec 111/10 and Lu 217/17.

References

[1] S. Scudino, U. Kühn, L. Schultz, D. Nagahama, K. Hono, J. Eckert, J. Appl. Phys. 95 (2004) 3397.
[2] A. Inoue, Acta Mater. 48 (2000) 279.
[3] L.Q. Xing, J. Eckert, W. Löser, L. Schultz, Appl. Phys. Lett. 74 (1999) 664.
[4] Z. Bian, G. He, G.L. Chen, Scripta Mater. 46 (2002) 407.
[5] L.Q. Xing, J. Eckert, L. Schultz, Nanostruct. Mater. 12 (1999) 503.
[6] S. Scudino, J. Eckert, U. Kuehn, H. Breitzke, K. Lueders, L. Schultz, MRS Symp. Proc. 806 (2004) 83.
[7] A. Inoue, T. Zhang, J. Saida, M. Matsushita, M.W. Chen, T. Sakurai, Mater. Trans. JIM 40 (1999) 1181.
[8] J. Eckert, N. Mattern, M. Zinkevitch, M. Seidel, Mater. Trans. JIM 39 (1998) 623.
[9] A. Gebert, J. Eckert, L. Schultz, Acta Mater. 46 (1998) 5475.
[10] D. Sordelet, X. Yang, E.A. Rozhkova, M.F. Besser, M.J. Kramer, Intermetallics 12 (2004) 1211.
[11] P.A. Bancel, P.A. Heiney, P.W. Stephens, A.I. Goldman, P.M. Horn, Phys. Rev. Lett. 54 (1985) 2422.
[12] U. Köster, U. Herold, Glassy Metals I, Springer-Verlag, Heidelberg, 1980, p. 225.
[13] U. Köster, Mater. Sci. Forum 235–238 (1997) 377.